Yttria-stabilized zirconia-aluminum matrix composites via ultrasonic additive manufacturing

Zhangxian Deng, M. Bryant Gingerich, Tianyang Han, Marcelo J. Dapino*

NSF IUCRC Smart Vehicle Concepts Center, Department of Mechanical and Aerospace Engineering, The Ohio State University, Columbus, OH 43210, USA

ABSTRACT

High-integrity ceramic-metal composites combine electrical, thermal, and corrosion resistance with excellent mechanical robustness. Ultrasonic additive manufacturing (UAM) is a low temperature process that enables dissimilar material welds without inducing brittle phases. In this study, multiple layers of Yttria-stabilized zirconia (YSZ) films are jointed between layers of Al 6061-H18 matrix using a 9 kW UAM system. UAM is advantageous over existing metal-ceramic composite fabrication techniques by continuously joining ceramics to metals at a speed of 2 m/min while requiring a moderate temperature that is 55% of the melting point of aluminum. The welding interface, which is found to include a 10 nm thick diffusion zone, is investigated using optical microscopy and energy-dispersive X-ray (EDX) spectroscopy. The shear strengths of the as-welded and heat-treated composites are 72 MPa and 103 MPa, respectively. The shear deformation and failure mechanism of the YSZ-Al composites are investigated via finite element modeling.

1. Introduction

Metals exhibit excellent machinability, high tensile strength, and conductivity (both electrical and thermal), but are vulnerable to corrosion. Ceramics, on the other hand, are refractory and corrosion resistant. Ceramics are also ideal for hard-wearing surfaces, electrical insulation, and thermal isolation. Ceramic-metal composites incorporating the merits of these two material types have been created to address complex engineering challenges [1]. Conventional fabrication techniques for ceramic-metal bonding include mechanical joining, indirect joining, and direct joining. Mechanical joining, such as press or shrink fitting, is suitable for mass production, but does not allow for complex geometries. Indirect joining utilizes binding materials including organic adhesives, glasses [2], and intermediate metals [3,4]. The limited wettability between the binding material and the ceramic surface greatly limits the bond strength.

Direct joining can be classified as fusion welding and solid-state welding depending on the process temperature. Fusion welding bonds metals with ceramics by melting and re-solidifying metallic materials on ceramic surfaces. The strength of the interface is constrained by the wettability. As the ceramic-metal joints cool down from the melting point (T_m) to room temperature, severe thermal stress exists due to the difference in coefficients of thermal expansion. The cooling procedure may also cause disruptive phase transformations and chemical reactions, which occur in the heat affected zone. Both the thermal stress and

the phase transformation weaken the welding interface. In contrast to fusion welding, solid-state welding is employed to bond metals with bulk ceramic pieces directly at a temperature below T_m. Diffusion joining, which is a typical solid-state welding technique, bonds dissimilar materials by pressing two flat and clean surfaces together under a temperature of 0.5–0.98 T_m for minutes or hours [5]. Due to the long duration and high temperature, a wide heat affected zone and residual stresses arise which weaken the interface strength. Friction stir welding is able to induce diffusion or plastic deformation between ceramics and metals within minutes at room temperature [6–9]. However, friction stir welding is not applicable for complex geometries, since uniform rubbing and heating on the interface are required.

Diffusion joining and friction stir welding require either long duration or high temperature to form strong ceramic-metal joints. Diffusion between ceramics and metals has recently been achieved in a short duration by applying a large normal compression and lateral ultrasonic vibrations on the interface. The ultrasonic vibrations are able to disperse oxide layers, remove contaminants, and collapse asperities on the interface thus resulting in solid-state bonding. Hence, the finish of welding surfaces is not critical. Woltersdorf et al. [10] first implemented ultrasonic welding to integrate alumina with Al. Due to numerous crystal defects, unbounded pores, and micro-cracks, the interface was shown to be mechanically weak. However, energy-dispersive X-ray (EDX) imaging suggested the possibility of creating diffusion via ultrasonic vibrations. Imai and Matsuoka [11]

---

experimentally welded Al on top of bulk alumina and zirconia base plates. The influence of input energy, welding pressure, surface roughness, and temperature was investigated. A mechanically-robust diffusion interface was achieved within two seconds by preheating the ceramic base plate to 200°C. Ultrasonic welding between ceramics and metals is feasible at room temperature by adding thin, ductile, and low-melting point metal films as binding materials. Wagner et al. [12] successfully welded steel to zirconia by inserting a thin layer of aluminum. A 2–10 nm thick joining zone was created at room temperature; mechanical tests showed a minimum tensile strength of 120 MPa. Matsuoka [13] utilized a 50 μm indium layer as the binding material and welded Al on bulk alumina or SiC base plates. Besides inserting thin metal films, binder materials have been applied on the welding surfaces via vapor deposition [14]. To avoid cracking of the ceramic layer, Ishikuro and Matsuoka [14] welded alumina and Al with reduced pressure and duration, although mechanical strength was sacrificed.

Following the principles of ultrasonic spot welding, ultrasonic additive manufacturing (UAM) provides an advanced method to build complicated geometries by layering up thin foils. This study for the first time achieves high strength diffusion bonding between metals and ceramics using a 9 kW UAM system. Multi-layer YSZ-Al composites are fabricated by alternately and continuously bonding thin YSZ films and Al foils at a speed of 2 m/min. Compared to existing direct joining techniques, summarized in Table 1, UAM exhibits a short welding duration of about 60 ms while requiring a moderate baseplate temperature of $0.55 \, T_m$. Details of the composite fabrication, as well as testing methods, are presented in Section 2. In Section 3, the consolidation quality of the YSZ/Al interface and bonding mechanisms are first investigated with micrography and EDX; the shear strength of the composites is experimentally quantified and numerically simulated.

2. Material and methods

2.1. Composite fabrication

UAM has been implemented to bond dissimilar thin metal foils (typically 152.4 μm thick) [15–17]. This study utilizes a 9 kW UAM system, as shown in Fig. 1, to embed thin ceramic films within a metal matrix. The system consists of an automatic metal tape feeder and a computer numerical control (CNC) stage. The lateral ultrasonic vibrations, at 20 kHz, are generated by a sonotrode connected to a pair of piezoelectric actuators. The sonotrode operates in a rolling action thus allowing for continuous welding.

Joining thin ceramic layers with metal base plates has traditionally been challenging due to the brittleness of ceramics. YSZ films manufactured by ENrG Inc., whose composition is presented in Table 2, exhibit reasonable flexibility and tolerate temperatures up to 1200 °C, making it an ideal material candidate for ceramic-metal composites. In

this study, thin ceramic films are directly bonded to Al 6061-H18 for the first time.

Fig. 2 shows the setup for fabricating YSZ-Al composites. A steel plate is held tightly on the UAM machine with a vacuum chuck. A 2.34 mm thick Al 6061-T6 baseplate is bolted to the steel plate. The steel plate and the Al base plate are initially heated up to 400 °F (204.4°C). Six layers of Al 6061-H18 with a thickness of 0.152 mm and a width of 25.4 mm are first welded on top of the base plate. A normal force of 4 kN and an ultrasonic vibration with an amplitude of 32 micron peak-to-peak are applied on the Al tape by the sonotrode. The welding speed for Al/Al welding, which is the travel speed of the base plate along the x-axis, is 200 inch/min (5.08 m/min). To enhance the vibration energy transferred to the interface, the sonotrode has a surface roughness of 14 micron RA which induces a texture on top of the Al layer. The top surface of the Al layer is machined flat to prevent cracking in the YSZ layer during YSZ-Al joining. A layer of 40 micron thick YSZ is laid over the machined surface. A large Al sheet instead of 25.4 mm wide Al 6061-H18 foils is implemented to securely constrain the YSZ during welding. Without the Al sheet, large portions of the YSZ will fracture and fly away from the weld zone during the weld pass. As shown in Fig. 2, the 0.152 mm thick Al 6061-H18 sheet is secured over the unwelded YSZ by pulling a vacuum. The vacuum both holds down the aluminum sheet and ensures that the YSZ film does not move during the welding. A normal force of 4 kN and an ultrasonic vibration with an amplitude of 30 microns are applied on the Al sheet via the sonotrode. The welding speed is 2.032 m/min. After welding the YSZ, 21 additional layers of 0.152 mm thick Al 6061-H18 foils are welded onto the Al sheet to build up enough material for shear testing. The obtained YSZ-Al composites containing a single layer of YSZ film are cut into 4.95 mm × 4.95 mm × 6.50 mm (0.195 inch × 0.195 inch × 0.256 inch) samples via the built-in CNC in the UAM machine, as shown in Fig. 3. Composites that contain two layers of YSZ films are also fabricated using the same welding parameters and procedures. The only difference is that an additional layer of 0.152 mm thick Al 6061-H18 was inserted between two YSZ layers.

Fig. 3 shows the shear samples, where three of the specimens were tempered to the T6 condition by solutionizing at 530 °C for 1 h, quenching in water, then aging at 160 °C for 18 h [20].

2.2. Micrography

The as-welded YSZ/Al interface is investigated qualitatively and quantitatively using microscopy analyses. Optical micrographs are attained from a microscope. Transmission electron microscope (TEM) and electron diffraction X-ray spectroscopy (EDX) are performed using a Tecnai F20 TEM with EDX capability. Optical imaging is performed to analyze the consolidation quality on the YSZ/Al interfaces. TEM imaging is done to locate the YSZ/Al interface; EDX line scans are

Table 1
Comparison of existing direct joining methods. (T_m: melting temperature of the metal; RT: room temperature).

| Methods	Temperature	Duration	Drawbacks
Fusion welding [3]	$> T_m$	minutes or hours	· Severe residual stress · Wide heat affected zone · Harsh requirement for wettability
Diffusion welding [5]	$0.5–0.98 \, T_m$	minutes or hours	· Requires flat and clean surfaces · Severe residual stress · Wide heat affected zone
Friction stir welding [6–9]	RT	minutes	· Not for complex geometries · Requires uniform rubbing and heating on the interface
Ultrasonic spot welding [12–14] (with binding layers)	RT	< 1s	· Soft and weak binding layers · Single layer bonding · Discrete welding locations
Ultrasonic spot welding [10,11] (without binding layers)	$0.5–0.6 \, T_m$	seconds	· Single layer bonding · Discrete welding locations
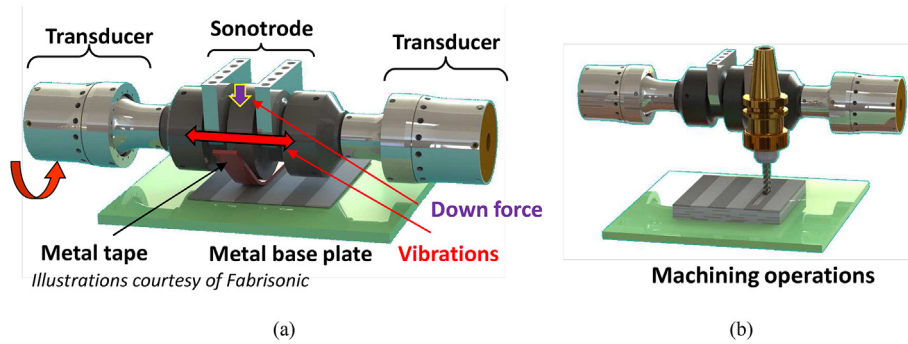
Fig. 1. Modern UAM system that operates within a CNC framework. (a) Ultrasonic welder assembly and (b) tooling for subtractive machining [18].

Table 2
Composition of the YSZ film utilized in this study [19]. (CaO, Fe, Si, and Ti are each less than 0.05 wt.%).

	ZrO_2	Y_2O_3	HfO_2	Al_2O_3
wt.%	83–95	4–15	1–2	0.1–0.5
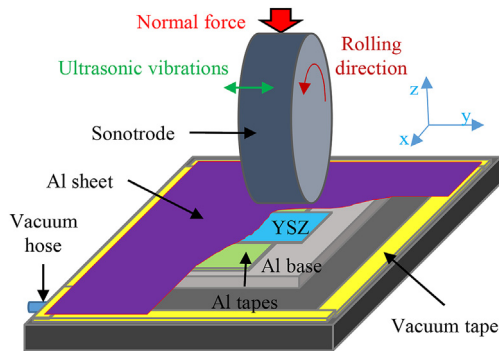
Fig. 2. Schematic of joining YSZ films on aluminum using ultrasonic additive manufacturing system.
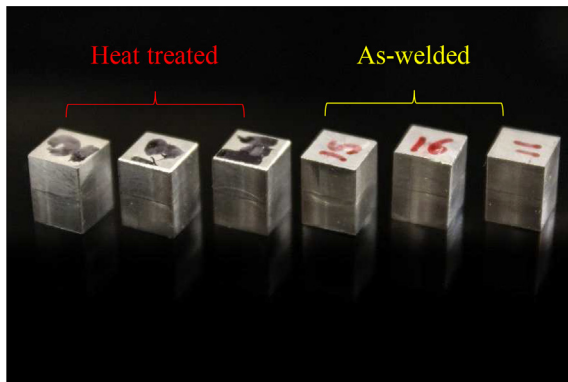

Fig. 3. As-welded and T6 heat treated YSZ-Al samples.

performed simultaneously across the interface to quantify diffusion.

The sample for optical imaging is cutout of the UAM welded sample using standard CNC milling operations. The surface of the sample is then polished using standard preparation methods, finishing with $1\,\mu m$ polishing compound. The TEM sample is cutout using a FEI Helios NanoLab 600 Dual Beam FIB/SEM. This sample is cut at the interface between the YSZ layer and the top aluminum foil layer. TEM imaging and EDX are completed using an electron acceleration voltage of 200 keV and probe size of less than 1 nm. The EDX scan distance is 50 nm.

2.3. Shear strength testing

The interfacial strength of UAM-fabricated composites is often characterized by peel and push-pin tests, but these tests cannot directly measure tensile or shear interfacial strength [21–23]. Thus, a custom shear test method is designed and tested in this study to characterize the absolute shear strength of the YSZ-Al interface, as shown in Fig. 4 (a).

The shear fixture is utilized in conjunction with an MTS C43.504 load frame and a pair of compression platens, as shown in Fig. 4(b). The load frame operates in displacement control mode and the crosshead speed is 1.2 mm/min (0.047 inch/min). The displacement is measured by a built-in position sensor with a resolution of $0.6\,\mu m$. The axial load is measured by a 20-bit, 50 kN range load cell with an accuracy of 13 N. Due to the relatively slow displacement rate, a sampling frequency of 10 Hz is selected to collect enough data points. The test is stopped at a maximum relative travel distance of 3 mm.

2.4. Shear strength modeling

In conjunction with shear testing, a two-dimensional finite element model is developed in Abaqus. The purpose of this model is to numerically quantify interfacial stresses and estimate the stress distribution in the composite. Fig. 5 presents the model configuration and mesh details. The model considers the elasticity and plasticity of the aluminum matrix. A boundary velocity of 1.2 mm/min is applied in the x direction to simulate the movement of the load frame. The top and bottom surfaces of the Al-YSZ composite are constrained in the y direction. The shear stress is calculated as $\tau = F_r/A_s$, where F_r is the reaction force on the fixture and A_s is the cross section area of the sample. The YSZ film is assumed to exhibit no plasticity and shear failure in the YSZ film is neglected. It is safe to ignore the brittleness of YSZ, because the YSZ layer is extremely thin and close-up optical images of the fracture surface show no evidence of shear cracks in YSZ. The shear failure is explained in greater detail in the following section. To efficiently and accurately describe the deformation behavior, a sweep mesh with at least three layers of elements is defined in the YSZ layer. The mesh is iteratively refined until the peak load calculation varies by no more than 2%.

We assume that the shear failure is initiated in the YSZ/AL interface. The thickness of the YSZ/Al interface is in the nano scale, which is dramatically thinner than other domains. Thus, a surface-based cohesive behavior is defined to describe the welding interface. The failure of the interface is defined by the maximum tensile stress σ_0 and the maximum shear stress τ_0. Before the initiation of damage, or when the stresses are within the defined stress boundaries, a linear elastic behavior is defined to relate normal and shear stresses to the normal and shear strains across the interface. Three stiffness values, which are the normal stiffness k_{nn}, the shear stiffness k_{ss}, and the torsional stiffness k_{tt}, are defined to describe the elasticity of the welding interface. The damage evolution of the YSZ/Al interface is assumed to be similar to that
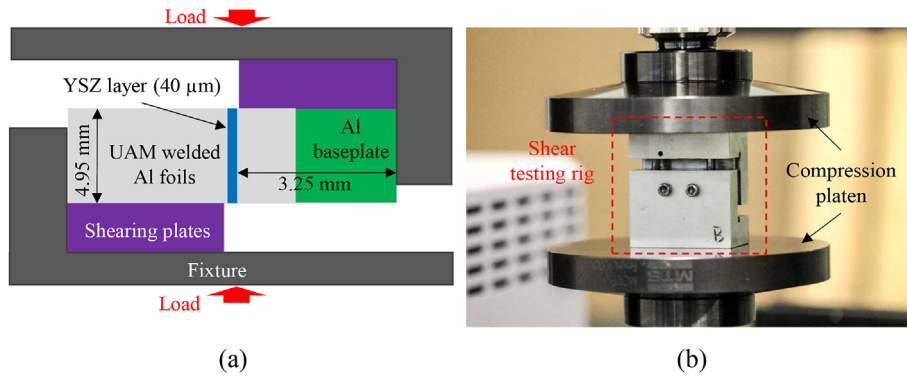
Fig. 4. (a) Shear test loading configuration and (b) shear testing setup on MTS load frame.
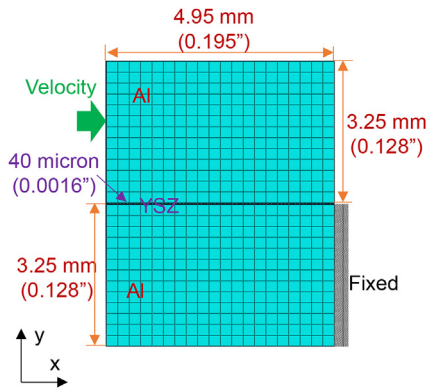

Fig. 5. Two-dimensional finite element model developed in Abaqus.

of ductile metals. Once the damage initiation criterion is reached, the damage is simulated as the progressive degradation of the material stiffness, which is described by a nonlinear plastic displacement u^{pl}. The shape of u^{pl} is defined by an evolution function as

$$d = \frac{1 - e^{-\alpha \frac{u^{pl}}{u_f^{pl}}}}{1 - e^{-\alpha}}, \tag{1}$$

where α is the exponent value, u_f^{pl} is the plastic displacement at failure, and d is the effective plastic displacement ranging from 0 to 1. This damage evolution definition is mesh-independent.

3. Results and discussion

3.1. Micrography

3.1.1. Optical imaging

Optical micrographs of the sample cross sections for as-welded YSZ-Al composites are presented in Fig. 6. Aluminum foil interfaces cannot be identified, demonstrating effective consolidation provided by UAM. Fig. 6(a) confirms that no voids are present at the bulk YSZ/Al interface when a single layer of YSZ film is built within the Al matrix. Preliminary welding trials have also demonstrated the possibility of creating alternating YSZ layers (20 μm thick) and Al layers, whose interfaces are analyzed using optical microscopy as shown in Fig. 6(b).

3.1.2. TEM and EDX

A line scan across the YSZ/Al welding interface was completed at the location shown in Fig. 7(a). The line scan was completed on an as-welded sample; no heat treatments were given to the sample prior to the EDX analysis. The aluminum appears dark near the YSZ/Al interface due to sample thinning for optimal EDX measurements. The YSZ-Al composites are fabricated through direct UAM welding and no chemical

reaction occurs at the welding interface. Thus, the composition of the welding interface is a transition of Al 6061 to YSZ. The composition through the weld zone can be quantified by tracking the atomic percentages of metallic elements, as shown in Fig. 7(b). The diffusion region, where the atomic percentages of Al and Zr show significant variation, is located in the 20–30 nm region. No Zr is found in the aluminum region, since aluminum has a much smaller lattice structure than zirconia. Y and Hf stay on the YSZ side of the interface and have negligible atomic percentages (less than 1%) in the diffusion region. This observation also confirms that YSZ does not diffuse into Al. The Al atoms diffuse into the YSZ region up to a depth of about 10 nm. The diffusion region shows a significant portion of Mg, up to 8%, which originates from the as-received Al 6061-H18 foils utilized in this study.

The probable cause for the unexpected atomic percentage of Al from 0 to 20 nm of the line scan is Zr L series X-rays fluorescing the Al. The Zr L X-ray energy is at 2.04 keV and the Al absorption edge is at 1.56 keV. When the X-ray energy is just above the absorption edge, it is strongly absorbed which then ionizes the absorber causing it to emit at its characteristic energy. In this case, the Zr atoms radiate isotropically and fluoresce the Al atoms. Consequently, some data smearing on the Al concentration measurement occurs within the YSZ region. This, however, does not nullify the transition zone at the YSZ/Al interface.

Diffusion between two dissimilar materials is typically induced by temperature, pressure, and time [5]. The YSZ-Al composites are fabricated at various base plate temperatures. Under the aforementioned welding parameters, bonding YSZ with Al is not possible at room temperature; weak joints are achieved around 300 °F (148.9 °C); strong joints are obtained when the base temperature is 400 °F (204.4 °C). The absolute melting point T_m of Al 6061-H18 is about 860.8 K (587.8 °C) and the welding temperature is about 0.55 T_m, which is at the lower end of the diffusion temperature range (0.5–0.98 T_m) reported in previous studies [2]. The welding speed is also much faster than previous diffusion welding [5], friction stir welding [6], and low power ultrasonic metal welding [11]. The bonding occurs in a fraction of a second and does not require special surface treatment. This experimental study indicates that high power ultrasonic vibrations on the interface induce high strain rates that may facilitate the diffusion of Al into YSZ.

3.2. Shear strength testing

Shear strength for as-welded and heat-treated samples are characterized by measuring the quasi-static shear stress versus displacement curves, as shown in Fig. 8. These samples are not utilized in the optical or microscopic imaging, but are fabricated simultaneously using the same welding conditions. The average shear strengths of as-welded and heat-treated samples are 72 MPa and 103 MPa, respectively. The mechanical strength of the ceramic-metal joints fabricated in this study is much higher than the values reported in the refs. [5–7]. Three of each sample type are tested, exhibiting consistent results. For heat-treated samples, the failure is abrupt; for as-welded samples, some of the failure
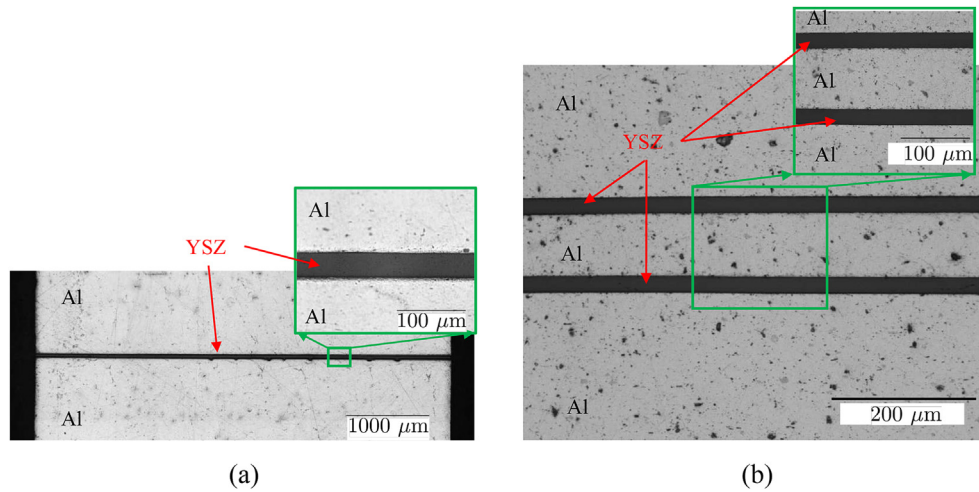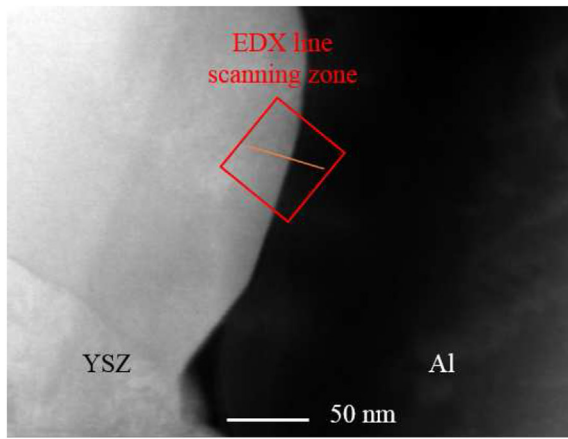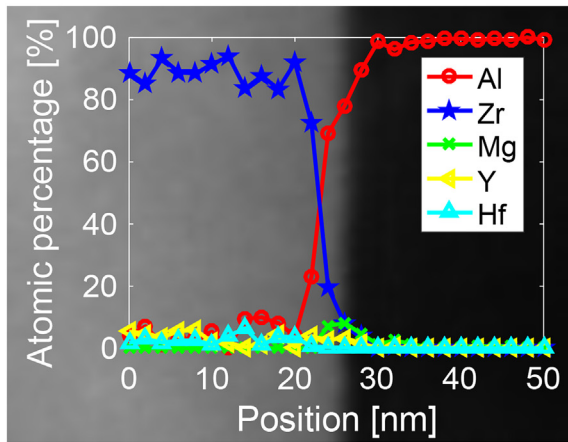
(a)

(b)

Fig. 6. (a) Optical micrograph across the width of the YSZ/Al welding interface on an as-welded shear sample and (b) optical micrograph showing two layers of YSZ films welded within an Al structure.

(a)

(b)

Fig. 7. (a) TEM image of the YSZ/Al welding interface and (b) EDX results showing the atomic percentages of metallic elements at the YSZ/Al interface. The sample used for the linescan was given no heat treatments prior to the EDX measurements.

is gradual. The gradual failure may have been caused by welding in-duced cracks within the YSZ layer, resulting in a stepped failure pro-gression.
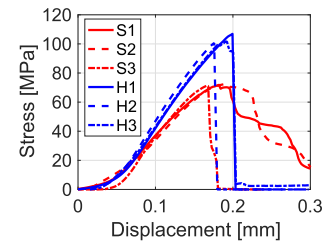

Fig. 8. Shear testing results (S: as-welded and H: HT to T6 heat treatment).

Fig. 9 shows the fracture surfaces of the as-welded and heat-treated YSZ-Al composites after shear tests. Part of the YSZ film stays on the bottom piece and the rest sticks to the top piece. The boundary on the top piece almost mirrors the bottom piece. The small difference in-dicates that some of the YSZ film cracks and falls off the sample. For the as-welded composite, machining marks due to milling can be found on the bottom aluminum matrix; white spots following the machining marks can be found in the YSZ region on the top piece, which is an indication of YSZ/Al diffusion. The aluminum matrix on the top piece has no machining marks but dark spots, which are due to the texture of the welding horn. The YSZ film breaks into two sections during shear testing; this is potentially due to imperfections or micro cracks existing in the as-welded composites. For the heat-treated composite, all of the YSZ film sticks to the top piece. This result shows that the heat treat-ment can partially revert imperfections and micro cracks. Clear white marks are imprinted on the YSZ film, which demonstrates an im-provement in YSZ/Al diffusion.

3.3. Shear strength modeling

The shear strength of the YSZ-Al composites is smaller than the strength of the aluminum matrix. Thus, the assumption that the failure is initiated at the YSZ/Al interfaces is reasonable. A global viscosity coefficient of 0.01 is added to the model for stabilization. The effective stiffness values associated with the welding interface are $k_{nn} = 1.40$ GN/m, $k_{ss} = 1.03$ GN/m, and $k_{tt} = 1.03$ GN/m for both types of composites. These values mainly affect the rising slope at the elastic region and are manually tuned to achieve a close fit. The damage initiation criteria and damage evolution parameters are summarized in Table 3.

Modeled shear stress versus displacement curves are presented on top of experimental results from as-welded and heat-treated samples in Fig. 10. The finite element model assumes an ideal force, which is perfectly parallel to the YSZ/Al interfaces of the composite. As a result,
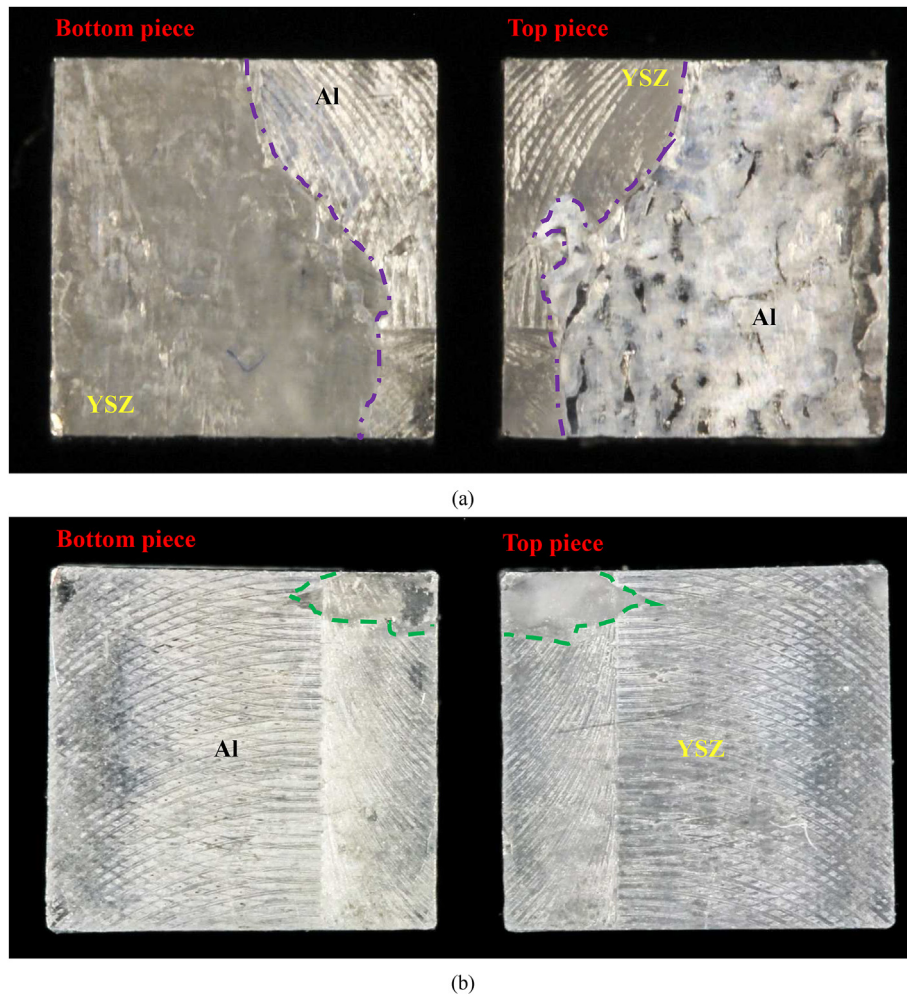
Fig. 9. Fracture surfaces of (a) as-welded and (b) heat-treated YSZ-Al composites. Purple lines illustrate the boundary between YSZ and Al; green lines illustrate the unbounded region. (For interpretation of the references to colour in this figure legend, the reader is referred to the Web version of this article.)

Table 3
Model parameters utilized for as-welded and heat-treated YSZ-Al composites.

	σ_0 [MPa]	τ_0 [MPa]	α [−]	u_f^{pl} [−]
As-welded	113.8	80.7	300	0.1
Heat-treated	136.5	113.1	200	0.05

the slope of the shear stress versus displacement curve remains constant. However, the initial slope of the experimental result gradually increases from 0 to a constant value. This varying slope is possibly introduced by the imperfect machining of the shear plates or the small-angle tilting of the sample during the shear testing. In Fig. 10, the initial slope change due to gradual loading is ignored and the modeling results are manually shifted by 0.026 mm and 0.045 mm, respectively, for as-welded and heat-treated samples.

4. Conclusion

High-integrity YSZ-Al composites are fabricated in this study utilizing ultrasonic additive manufacturing. The high strain rate introduced by ultrasonic vibrations may facilitate diffusion between ceramics and metals at a relatively low temperature and a very short weld duration. The mechanical strength of the welding interface is much higher than it is for friction stir welding and diffusion welding. The mechanical strength of the interface can be further improved via
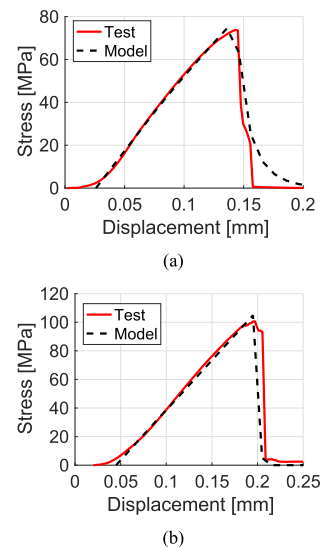

Fig. 10. Comparison of experimental results and finite element results for (a) as-welded and (b) heat-treated composites.

heat treatment. Unlike previous ultrasonic welding methods, multiple layers of thin ceramic layers are built inside metal structures for the first time. Hence, composites with alternating ceramic and metal layers are

available for future applications that require anisotropic thermal or electrical conductivity. Previous studies have also suggested that the interface strength can be further improved via annealing [24]. Future studies will aim to enhance composite strength via other heat treatments (e.g., annealing, hot isostatic pressing).

Acknowledgments

Appendix A. Supplementary data

Supplementary data related to this article can be found at http://dx.doi.org/10.1016/j.compositesb.2018.06.001.

References

[1] Loehman RE. Characterization of ceramics. Momentum Press; 2010.
[2] Nicholas M, Mortimer D. Mater Sci Technol 1985;1:657–65.
[3] Uday M, Ahmad-Fauzi M, Noor AM, Rajoo S. Joining Technologies vol. 8. 2016.
[4] Zhang P, Fang J, Fu R, Gu X, Fei M. Mater Des 2015;87:619–24.
[5] Nicholas M, Crispin R. J Mater Sci 1982;17:3347–60.
[6] Fauzi MA, Uday M, Zuhailawati H, Ismail A. Mater Des 2010;31:670–6.
[7] Uday M, Fauzi MA, Zuhailawati H, Ismail A. Mater Sci Eng 2011;528:1348–59.
[8] Fernie J. Mater Manuf Process 1994;9:379–94.
[9] Uday M, Fauzi MA, Zuhailawati H, Ismail A. Mater Sci Eng 2011;528:4753–60.
[10] Woltersdorf J, Pippel E, Roeder E, Wagner G, Wagner J. Phys Status Solidi A 1995;150:307–17.
[11] Imai H, Matsuoka SI. JSME Int J Ser A 2006;49:444–50.
[12] Wagner G, Balle F, Eifler D. JOM (J Occup Med) 2012;64:401–6.
[13] Matsuoka SI, Mater J. Process. Technol 1994;47:185–96.
[14] Ishikuro T, Matsuoka SI. JSME Int J Ser. A 2005;48:317–21.
[15] Sriraman M, Babu S, Short M. Scripta Mater 2010;62:560–3.
[16] Gunduz IE, Ando T, Shattuck E, Wong PY, Doumanidis CC. Scripta Mater 2005;52:939–43.
[17] Sridharan N, Wolcott P, Dapino M, Babu S. Scripta Mater 2016;117:1–5.
[18] Hehr A, Dapino M. Composites Part B 2015;77:199–208.
[19] https://www.enrg-inc.com/products.
[20] Wolcott PJ, Pawlowski C, Headings LM, Dapino MJ. J Manuf Sci Eng 2017;139:011010.
[21] Kong CY, Soar RC, Dickens PM. Sci Technol Mater Sci Eng A 2003;363:99–106.
[22] Zhang CS, Deceuster A, Li L. Sci Technol J Mater Eng Perform 2009;18:1124.
[23] Wolcott PJ, Hehr A, Dapino MJ. J Mater Res 2014;29:2055–65.
[24] Singh G, Yu Y, Ernst F, Raj R. Acta Mater 2007;55:3049–57.